MASSIVE STAR FORMATION NEAR THE SUPERNOVA REMNANT W30

P. Ojeda-May

Facultad de Ingeniería, Universidad Autónoma de Yucatán

S. E. Kurtz, L. F. Rodríguez, S. J. Arthur

Instituto de Astronomía, Universidad Nacional Autónoma de México, Campus Morelia

and

P. F. Velázquez

Instituto de Ciencias Nucleares, Universidad Nacional Autónoma de México

RESUMEN

Presentamos observaciones del radiocontinuo a 6 cm (con una resolución de 1 segundo de arco) de sitios candidatos a ser regiones de formación estelar, los cuales se encuentran situados alrededor del remanente de supernova W30. Se detectó un total de nueve fuentes, algunas de las cuales pueden ser regiones H II ultracompactas. Una de estas fuentes, la G8.139−0.026, tiene una forma cometaria. De las ocho fuentes *IRAS* observadas, sólo tres tienen fuentes en radio continuo cercanas ($< 1''$). La baja tasa de detección de contrapartes en radio de las fuentes *IRAS* sugiere que W30 es un remanente joven que puede haber iniciado el proceso de formación estelar (lo cual es indicado por la presencia de fuentes en infrarrojo), pero este proceso de formación aún no ha concluido (lo cual parece estar de acuerdo con la falta relativa de contrapartes en el radiocontinuo).

ABSTRACT

We present arcsecond-resolution 6 cm continuum observations of potential massive-star formation sites in the vicinity of the W30 supernova remnant. Nine sources are detected, several of which could be ultracompact H II regions. One of these, G8.139−0.026 has a cometary morphology. Of the eight *IRAS* sources observed, only three have nearby ($< 1'$) radio continuum sources. The low detection rate of continuum counterparts for the *IRAS* sources suggests that this relatively young supernova remnant may have initiated massive star formation, as indicated by the presence of infrared sources, but there has been insufficient time for the formation process to finish, as indicated by the dearth of radio continuum sources.

1. INTRODUCTION

Supernova-induced star formation was first suggested by Öpik (1953). Subsequently a number of studies have examined many aspects of the supernova-interstellar medium interaction and the possibility of induced star formation, including Jura (1976), Woodward (1976), Krebs & Hillebrandt (1983), Herbst & Assousa (1977), Assousa, Herbst, & Turner (1977), and Junkes, Fürst, & Reich (1992). Many of the observational efforts seeking a supernova remnant (SNR) interaction with the interstellar medium (ISM) have focused on expanding shells of gas. In this paper we concentrate on recently formed stars, as traced by ultracompact H II regions.

The energy released by a supernova can heat dust in the nearby ISM, resulting in emission at far-infrared wavelengths (e.g., Arendt 1989). Rengarajan, Verma, & Iyengar (1989) found a significant excess of *IRAS* point sources associated with SNRs and suggest that these are dusty knots heated by SNR shocks. *IRAS* point sources whose colors correspond to those of ultracompact H II regions (Wood

& Churchwell 1989a, hereafter WC89a) may represent sites of recent massive star formation that was induced by the passage of a SNR shock. To test this hypothesis, and to study the interaction of SNR with the ambient ISM, we made observations of potential massive star formation sites in the vicinity of the W30 (G8.7−0.1) SNR.

W30 was identified as a SNR by Odegard (1986), who noted its unusual radio morphology. The relation of the thermal and non-thermal emission found in the region was greatly clarified by Kassim & Weiler (1990, hereafter KW90) who reported 90 cm and 20 cm Very Large Array (VLA) observations. Higher resolution VLA observations at 90 cm and of the H I line were reported by Frail, Kassim, & Weiler (1994). Frail et al. discuss the possible association of the W30 SNR with the pulsar PSR 1800–21, as do Finley & Ögelman (1994) who present *ROSAT* observations of the pulsar and the remnant. The remnant is roughly circular, approximately 45′ in diameter, and has a number of foreground H II regions toward the south. Numerous *IRAS* sources are found in the vicinity.

There has been considerable discussion regarding the distance to W30 but a frequently cited value is 6 ± 1 kpc, based on kinematic distances to the H II regions and the Σ-D relation for supernovae (see Odegard 1986, KW90, and Frail et al. 1994). Finley & Ögelman (1994) point out that more recent galactic rotation models applied to the H II regions suggest a near kinematic distance of about 4.8 kpc. This is consistent with the molecular gas distance, traced by CS observations of *IRAS* sources bordering the SNR (Bronfman, Nyman & May 1996). We adopt a distance of 5 kpc for the *IRAS* and radio sources found in the immediate vicinity of W30. At this distance, the SNR has a linear diameter of about 65 pc. Odegard (1986) estimated the remnant age to be 15,000 years.

2. SOURCE SELECTION

Nine fields near the W30 SNR were observed; all were considered to be likely massive-star formation sites because of their large *IRAS* fluxes (typically over 1000 Jy at 100 microns) and/or their far-infrared colors or possible association with H II regions. We observed the five H II regions designated A–D and G in the nomenclature of KW90. Three of these (A, B and G) have *IRAS* sources located very near the positions given in KW90. We also observed four additional *IRAS* sources (see below). The pointing center for each of the nine fields is given in Table 1, along with the corresponding

IRAS source and/or H II region designation. The H II region designated F by KW90 was not a target of these observations. It was detected nonetheless, albeit very far outside the primary beam (see § 4.7).

Using the 327 MHz VLA image of W30 (Frail et al. 1994), we estimate the geometric center of the SNR to be (B1950) $\alpha = 18^{\rm h}02^{\rm m}30^{\rm s}, \delta = -21°32'00''$. Eight *IRAS* sources within 1° of this position satisfy the WC89a color criteria; six of these are included in our sample (in fields 1, 3 and 5–8). Of the two *IRAS* sources with WC89a colors that we did not observe, 18032−2137 and 18048−2131, the former was observed by Wood & Churchwell (1989b), who reported the UC H II region G8.67−0.36. For the latter, Bronfman et al. (1996) report a CS detection but Codella et al. (1995) do not report water masers to a detection limit of 5.7 Jy. We note that 18043−2153 (field 9) marginally fails the WC89a F_{25}/F_{12} criterion, while 18016−2148 (field 2), though coincident with the KW-B position, does not satisfy the WC89a criteria.

3. OBSERVATIONS AND DATA REDUCTION

The observations were made on 1994 July 22, using the Very Large Array of the NRAO[1]. The array was in the B configuration, but the inner antennas of each arm were in use for a separate observational program. The outermost 17 antennas used for these observations provided baseline lengths from 0.3 to 10 km. At the observing frequency of 4.86 GHz, the *uv* coverage provided an angular resolution of approximately $2'' \times 1''$, and sensitivity to structures up to about $40''$ in size. On-source observation times were about 10 min, using a 100 MHz bandwidth and observing both right- and left-hand circular polarizations. The absolute amplitude calibrator was 1328+307 (7.486 Jy) and the phase calibrator was 1730−130, with a bootstrapped flux density of 4.53 Jy. The data were calibrated, edited and imaged using standard procedures of the AIPS software package of NRAO. The maps were corrected for primary beam attenuation. The correction was typically $\lesssim 15\%$.

4. RESULTS

Nine sources were detected above the 5σ level. Their observed parameters are reported in Table 2. Field number 8 had no source above the 5σ detection level of 0.6 mJy. Two sources were detected in field 4. One of these, G8.375−0.346, was also detected near

TABLE 1

FIELDS OBSERVED

| | Pointing Center | | |
Field	$\alpha(1950)$	$\delta(1950)$	Related Source[a]
1	18 00 00.0	-21 48 06	17599$-$2148, KW-A
2	18 01 33.0	-21 48 45	18016$-$2148, KW-B
3	18 02 33.0	-21 52 45	18026$-$2153, KW-C
4	18 02 44.0	-21 49 13	KW-D
5	18 03 37.0	-21 26 50	18035$-$2126, KW-G
6	18 00 57.0	-21 55 44	18009$-$2155
7	18 02 46.0	-22 02 16	18027$-$2202
8	18 02 53.0	-20 59 28	18028$-$2059
9	18 04 23.0	-21 53 27	18043$-$2153

[a]Designations are *IRAS* sources and KW90 H II regions.

the center of field 3. The other, G8.668$-$0.355 is approximately 14′ from the field center. Effectively, then, field 4 was also null at the 5σ level.

4.1. *G8.139$-$0.026*

This cometary H II region coincides with IRAS 18009$-$2155 (see Fig. 1). The infrared luminosity (assuming a distance of 5 kpc) is $1.2 \times 10^4 \, L_\odot$, indicative of a B0.5 ZAMS star. It is reported in the galactic plane survey (GPS) of Becker et al. (1994) and Zoonematkermani et al. (1990) as G8.140$-$0.027. Our measured flux density of 60.7 mJy is slightly higher than the Becker et al. value of 52.1 mJy. Given the 1.4 GHz flux density of 44 mJy from Zoonematkermani et al., the spectral index is $+0.2 \pm 0.1$, indicating thermal free-free emission. The integrated flux density of the source implies an electron density of about 3000 cm^{-3} and an excitation parameter of 17. The emission measure is about 10^6 pc cm^{-6}. An ionizing photon flux at least equivalent to that of a B0 star is required to maintain the ionization. Interestingly, Bronfman et al. (1996) did not detect molecular gas coincident with this *IRAS* position. This would seem to suggest that the absence of CS emission in their survey does not necessarily imply the absence of an H II region. No emission is seen in the NVSS map which suggests that this source is not part of a more extended H II region.

It is somewhat unusual that the spectral type indicated by the infrared emission (B0.5) is later than that indicated by the radio emission (B0). This may suggest that there is relatively little dust within the H II region and/or that the star is relatively isolated, without the cluster of lower-mass stars that is normally found accompanying a massive star. Using the

G8.139-0.026 **6 cm**

Continuum peak brightness = 6.87 milliJy/beam
Levels = 68.7 microJy/beam * (-10, 10, 20, 30, 40, 50, 60, 70, 80, 90)
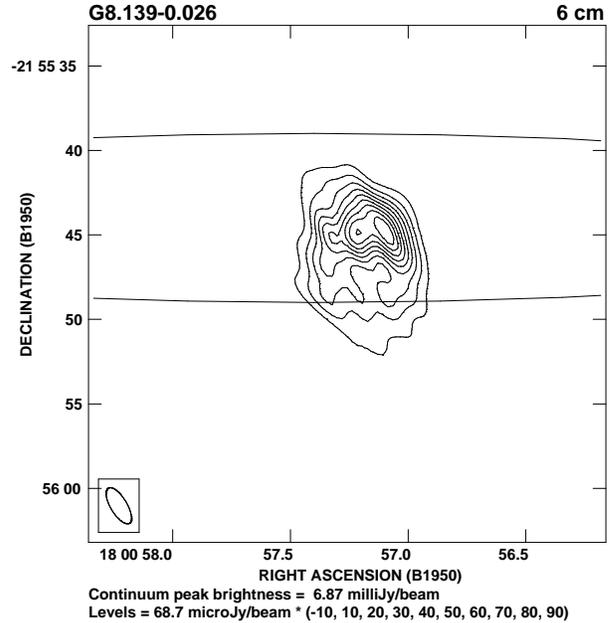
Fig. 1. Our 6 cm VLA image of the G8.139$-$0.026 region. The peak brightness and contour levels are indicated below the figure; the synthesized beam is shown in the lower left corner. The two nearly horizontal lines are the visible portion of the *IRAS* uncertainty ellipse of 18009$-$2155.

lower flux density of 52.1 mJy does not significantly change the spectral type estimate based on the radio flux density.

4.2. *G8.139+0.223 and G8.142+0.237*

The dominant source in field 1 is G8.14+0.22, shown in the NVSS image (Condon et al. 1998) of Figure 2. This source is too large to be imaged by our observations. By eliminating the shortest 20 kλ baselines, we were able to suppress the extended emission and identify two compact sources, shown as stars in Figure 2. The integrated flux density of the NVSS map is 6 Jy, which implies a minimum ionizing photon rate of $10^{49.16}$ s^{-1}, corresponding to a ZAMS O6 star. The 17599$-$2418 luminosity is $2.5 \times 10^5 L_\odot$ which also corresponds to an O6 (single star) spectral type.

G8.139+0.223 is nearly coincident with the peak of G8.14+0.22 and also with IRAS 17599$-$2148 (RAFGL 2051; ellipse in Fig. 2). This source is reported as G8.14+0.23 by Wood & Churchwell (1989b); as G8.1390+0.2278 by Walsh et al. (1998); and as G8.139+0.224 by Becker et al. (1994). The maps of Wood & Churchwell and Walsh et al. do not agree with each other or with our own 6 cm map (not shown). Because of the imaging problems involved when both extended and compact emission

TABLE 2

DETECTED RADIO SOURCES

Radio Source[a]	α (1950)	δ (1950)	Flux Density S_{6cm} (mJy)[b]	Deconvolved Size ($''$)[c]	Synthesized Beam ($''$)	Map rms (mJy beam^{-1})
G8.139−0.026[6]	18 00 57.08	−21 55 44.9	60.7	13 × 9	2.64 × 0.98	0.17
G8.139+0.223[1]	18 00 00.86	−21 48 18.8	29.1	1.8 × 1.7	2.05 × 0.97	1.1
G8.142+0.237[1]	17 59 58.19	−21 47 43.2	89.8	4.6 × 2.9	2.05 × 0.97	1.1
G8.283−0.471[7]	18 02 55.54	−22 01 26.2	1.1	< 1.8	3.09 × 1.08	0.15
G8.338−0.093[2]	18 01 37.53	−21 47 21.0	38.9	< 0.7	1.88 × 0.91	0.28
G8.375−0.346[3]	18 02 39.14	−21 52 55.0	3.2	3.2 × 1.9	2.35 × 1.79	0.20
G8.563−0.681[9]	18 04 18.52	−21 53 02.4	4.2	< 1.0	2.99 × 0.96	0.14
G8.668−0.355[4]	18 03 18.68	−21 37 54.7	> 40[d]	∼ 8 × 2	2.71 × 2.06	0.25
G8.900−0.325[5]	18 03 41.40	−21 24 53.9	2.7	< 1.1	2.25 × 0.96	0.20

[a]The numeric superscript indicates the field number (c.f., Table 1) in which the source was observed.

[b]Estimated uncertainties are about 10% unless otherwise noted.   [c]FWZI

[d]Source is > 14$'$ from field center; primary beam correction factor cannot be accurately determined.

are present in the field, we do not derive physical parameters and we advise that the published radio data on this source should be treated with caution. High quality maps with spatial sensitivity from $\lesssim 1''$ to $\gtrsim 1'$ are a prerequisite for a proper study of this region.

G8.142+0.237 is $\sim 50''$ to the NW of the *IRAS* position and the NVSS peak. It appears to have a distinct morphology, as opposed to an "irregular" morphology that might occur if the source structure were dominated by imaging artifacts. It may be an UC H II region, and under this assumption we calculate $n_e \sim 5000$ cm^{-3}, $U = 20$, emission measure of 3×10^6 pc cm^{-6}, and a minimum ionizing photon rate equivalent to a B0 star. We reiterate, however, that multi-spatial scale maps are needed before sources in this field can be studied with confidence.

4.3. *G8.283−0.471*

This source is 2.5 from the IRAS 18027−2202 position, hence the radio and infrared sources are almost certainly unrelated. The radio source is weakly detected (6σ) and unresolved. We found no prior detection of G8.283−0.471 reported in the literature, and we consider its nature to be undetermined.

Perhaps more interesting than the radio source itself is the lack of centimeter continuum emission coincident with the *IRAS* position. If 18027−2202 is 5 kpc distant, then the IR luminosity is about $10^4 L_\odot$, corresponding to a B0.5 star. A resulting classical (spherical, uniform, optically thin, 10^4 K) H II region would have a flux density of ~ 6 mJy.
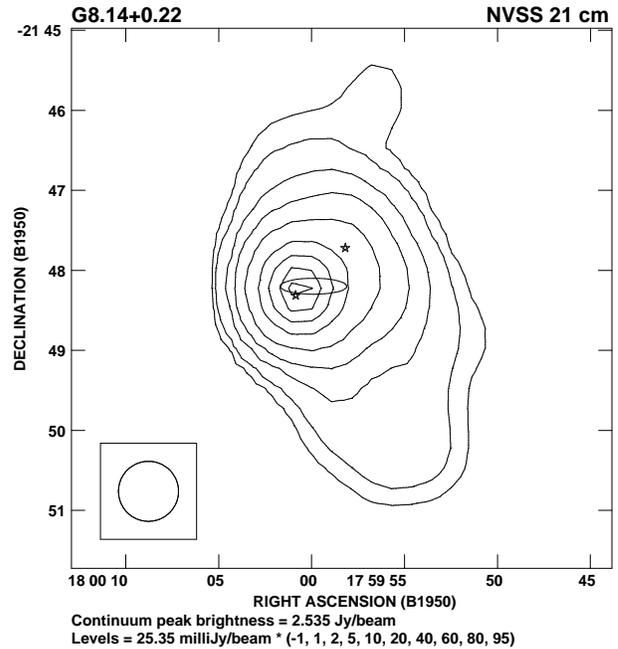
Fig. 2. The NVSS 21 cm image of G8.14+0.22. The peak brightness and contour levels are indicated below the figure; the synthesized beam ($45''$) is shown in the lower left corner. The peak of the continuum emission coincides with the uncertainty ellipse of IRAS 17599−2148. The two star symbols indicate the unresolved sources that we detect at 6 cm. G8.139+0.223 is nearly coincident with the *IRAS* source and the peak of the 21 cm emission, while G8.142+0.237 is about $50''$ to the NW.

Dust absorption of UV photons, optical depth effects, etc., might reduce this value below our 5σ detection level of 0.75 mJy. Source confusion within

the *IRAS* beam may result in an overestimate of the spectral type of the star (or most massive member of a cluster) in which case the expected 6 cm flux density would be even lower, making the lack of detection by our observations more likely. Molecular emission was not detected by the Bronfman et al. (1996) CS survey, and together with the lack of detected free-free emission this suggests that 18027−2202 is probably not an UC H II region, its *IRAS* colors (see § 4.6) notwithstanding.

4.4. *G8.338−0.093*

We detect a point source, offset about 10″ from the emission peak of the NVSS map (see Figure 3). This source is reported as G8.339−0.093 in the GPS of Zoonermatkermani et al. (1990) and Becker et al. (1994). Their 6 cm flux density of 36.2 mJy is in reasonable agreement with our value of 38.9 mJy. The NVSS core component (without the southern and western low level emission) is 344 mJy, somewhat larger than the 267 mJy reported by Becker et al., and suggesting that the source is variable. The source has a non-thermal spectrum between 90 and 6 cm, indicating that it is not an H II region. A more complete discussion is presented in Velázquez et al. (2002).

4.5. *G8.375−0.346*

This relatively weak radio source is located 23″ to the NE of the nearest *IRAS* source, 18026−2153 (see Figure 4). The radio source, if it is an H II region, would have a rather low electron density of about 600 cm^{-3} and the ionization could be provided by a B1 ZAMS star. It is unclear if the radio and *IRAS* sources are physically related. The luminosity of 18026−2153 (at 5 kpc) is 9×10^4 $L_\odot$, corresponding to a single-star spectral type of O7.5. Molecular gas was detected at the *IRAS* position by Bronfman et al. (1996). Using their CS velocity and the galactic rotation model of Wouterloot et al. (1990) indicates near/far kinematic distances of 3.8 and 4.8 kpc, corresponding to infrared luminosities of 5.2 and 8.3 $\times 10^4$ $L_\odot$, or spectral types of O8.5 and O7.5. Regardless of which distance is adopted, the *IRAS* data indicate the presence of a massive star. The lack of centimeter continuum emission coincident with such high luminosity sources has been discussed by Carral et al. (1999), who note that such sources are good candidates to search for thermal radio jets.

4.6. *G8.563−0.681*

We detect G8.563−0.681 as a point source 67″ to the NW of IRAS 18043−2153. No emission is seen in

G8.33-0.09   **NVSS 21 cm**

Continuum peak brightness = 258.8 milliJy/beam
Levels = 2.588 milliJy/beam * (-5, 5, 10, 20, 40, 60, 80, 98)
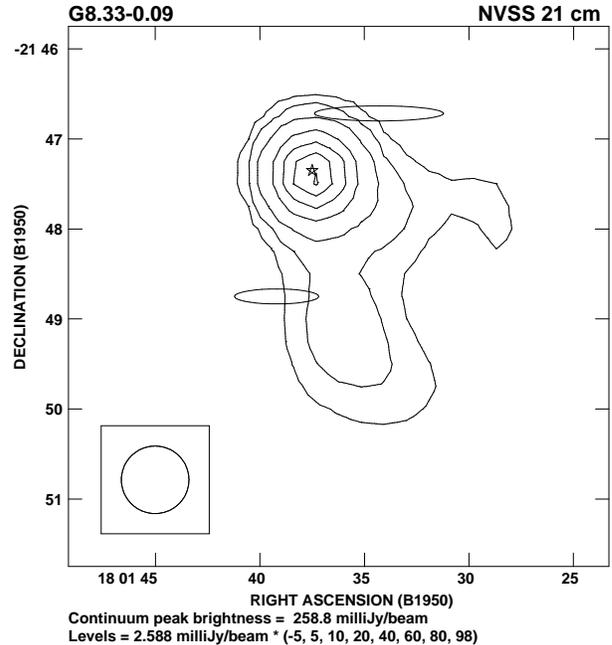
Fig. 3. The NVSS 21 cm image of the G8.33−0.09 region. The peak brightness and contour levels are indicated below the figure; the synthesized beam (45″) is shown in the lower left corner. Two *IRAS* uncertainty ellipses are shown, corresponding to 18016−2148 and 18015−2146. The star symbol, nearly coincident with the peak of the 21 cm emission, indicates the position of G8.338−0.093, which we detect but do not resolve at 6 cm.

the NVSS map at either the radio or *IRAS* position. At a distance of 5 kpc 18043−2153 would have a luminosity of 3.2×10^4 $L_\odot$, indicating an O9.5 ZAMS star.

WC89a proposed that *IRAS* colors $\log(F_{60}/F_{12}) \geq 1.30$ and $\log(F_{25}/F_{12}) \geq 0.57$ identify probable UC H II regions. The source 18043−2153 satisfies the first of these but marginally fails the second, with a value of 0.48. MacLeod et al. (1998) did not detect 6.7 GHz methanol maser emission associated with the *IRAS* source, nor did Palla et al. (1991) detect water maser emission. Given the lack of maser emission and the partial (dis)agreement with the Wood & Churchwell color criteria, we consider it unlikely that 18043−2153 is a massive young stellar object.

4.7. *G8.668−0.355*

This source coincides with the H II region designated F by KW90. It is the G8.67−0.36 UC H II region reported by Wood & Churchwell (1989b) who associate it with IRAS 18032−2137. More recent observations are reported by Walsh et al. (1998). Because the source is so far ($\sim 14'$) from the pointing center of our observations (the KW90 region D) we

G8.375-0.346　　　　　　　　　　　　**6 cm**

Continuum peak brightness = 1.74 milliJY/beam
Levels = 17.4 microJy/beam * (-30, 30, 50, 70, 90)
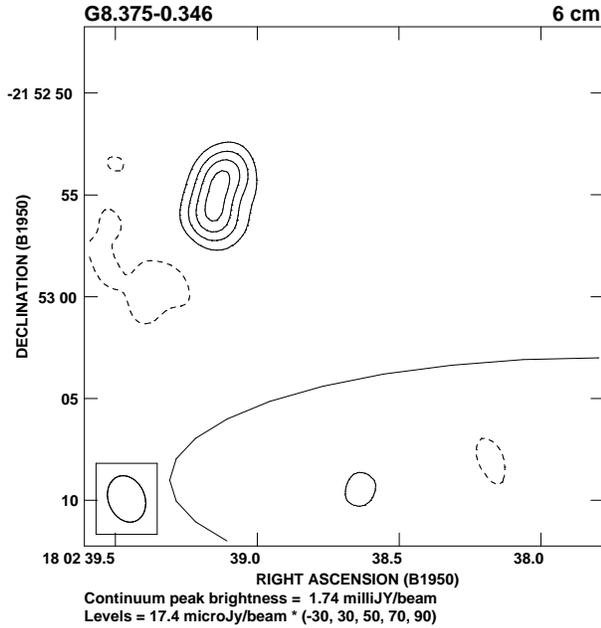
Fig. 4. Our 6 cm VLA image of the G8.375−0.346 region. The peak brightness and contour levels are indicated below the figure; the synthesized beam is shown in the lower left corner. The partial uncertainty ellipse of IRAS 18026−2153 is seen in the lower right. G8.375−0.346, of unknown nature, is about $23''$ to the NE of the *IRAS* position.

are not able to map it with confidence. We refer the reader to Wood & Churchwell and Walsh et al. for further details. Velázquez et al. (2002) note that various maser transitions in the F H II region have very nearly the same velocity as the supernova remnant, and interpret this as evidence for a possible interaction between the SNR and the H II region.

G8.668−0.355 is detected by the NVSS observations, as is a second source, G8.663−0.344, $50''$ further west. The fact that neither Wood & Churchwell nor Walsh et al. report the second source suggests that it is non-thermal.

We do not detect radio emission near the center of field 4, corresponding to the source KW-D. Inspection of the Altenhoff et al. (1978) map indicates that component D is somewhat weaker and more diffuse than the other H II regions noted in KW90. Our observations are sensitive to relatively bright, compact sources, which seem to be absent from this field.

4.8. *G8.900−0.325*

This source was detected in field number 5, which was centered on the *IRAS* source 18035−2126 and the KW-G H II region. G8.900−0.325 is nearly $2'$ distant from the field center, hence it seems unlikely to be physically related to either the *IRAS* source or

the KW-G region. We found no prior detection of G8.900−0.325 reported in the literature; we consider its nature to be unknown.

The NVSS map of this field shows a 490 mJy source (G8.868−0.319) coincident with 18035−2126. The source diameter is $\gtrsim 75''$, which is larger than can be imaged by our observations. Molecular emission is reported by Bronfman et al. (1996) and the near kinematic distance is 4.9 kpc, using the model of Wouterloot et al. (1990). Adopting the 5 kpc distance results in an *IRAS* luminosity of $3.6 \times 10^4 \, L_\odot$, or a single-star ZAMS spectral type of O9.5. A single-dish 4.875 GHz flux density of 640 mJy is reported by Wink, Altenhoff & Mezger (1982; for source G8.865−0.323). The resulting spectral index is +0.2, suggesting thermal free-free emission.

5. DISCUSSION

We observed six *IRAS* sources meeting the WC89a color criteria and detect nearby radio continuum emission in three of these. Two additional sources, with colors suggestive of star formation but failing the WC89a criteria, were also observed. The 50% detection rate we obtain (for sources meeting the WC89a criteria) is somewhat lower than the 80% detection rate reported by Kurtz, Churchwell, & Wood (1994) for similar *IRAS* sources (i.e., WC89a colors and locations toward the galactic center). A possible explanation for this is that if the SNR is about 15,000 yr old, as suggested by Odegard (1986), then there may not have been sufficient time for the star formation process to complete, and for the resulting massive star to produce an H II region. The three *IRAS* sources for which we do not detect radio continuum emission (IRAS 18027−2202, IRAS 18043−2153, and IRAS 18035−2126) may be good candidate massive protostars. In fact, if the SNR *is* this young, it is doubtful if *any* of the sources we detect represent massive stars whose formation was induced by the interaction of the SNR with the ambient ISM. It is possible that multiple massive-star formation sites were present in a molecular cloud complex and the SNR seen here is the first star in the cloud to become a supernova. If the W30 SNR is indeed only 15,000 yr old, then the presence of *IRAS* sources with WC89a colors and the *absence* of associated radio continuum emission would be evidence for SNR-induced star formation.

At first glance, Figure 5 suggests that there is relatively good coincidence between the radio and infrared sources. All the radio sources except the non-thermal source G8.338−0.093 appear to be located in close proximity to an *IRAS* source. This is
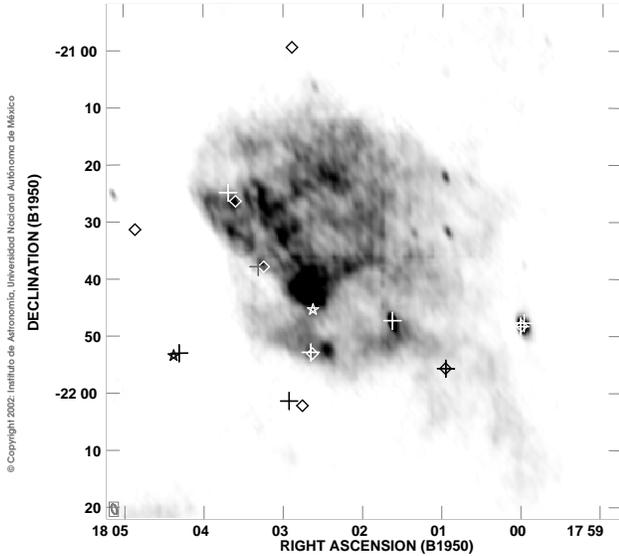
Fig. 5. The greyscale (5 to 350 mJy beam^{-1}) shows the 327 MHz image of the W30 supernova remnant of Velázquez et al. (2002). The nine crosses indicate the radio sources detected by our observations. The eight diamonds denote *IRAS* sources with Wood & Churchwell (1989a) colors. The two stars show *IRAS* sources which marginally fail one of the Wood & Churchwell colors.

slightly misleading, however, because of the scale of the map. Four of the seven "near coincidences" are actually about 1–3′ apart. We also stress that our observations—at a single wavelength—cannot confirm the thermal nature of the emission. At least one source, G8.338−0.093 is almost certainly non-thermal, and several of the other point sources may be non-thermal as well. Massive stellar winds, if present, would contribute only slightly to the flux densities we measure. At a distance of 5 kpc a mass loss rate of 10^{-5} $M_\odot$ yr^{-1} would produce a 6 cm flux density of several tenths of a milliJansky (e.g., Abbott et al. 1980).

There has been considerable discussion in the literature concerning the age of the W30 SNR and its possible association with the pulsar PSR 1800−21 (e.g., Odegard 1986, KW90, Frail et al. 1994, and Finley & Ögelman 1994). The age of the pulsar is estimated at 16,000 yr (Taylor, Manchester, & Lyne 1993). The age of the SNR is less certain, being based on the Σ-t relation of Caswell & Lerche (1979); the estimated age is also 15,000 yr (Odegard 1986). If the remnant is indeed only 15,000 yr old, then, with a diameter of about 65 pc, it is large for its age. The Vela SNR, for example, has roughly the same age but is only about half as large. An extremely low-density medium might ex-

plain the relatively rapid expansion of the remnant. There is supporting evidence for such low density gas. Finley & Ögelman (1994) derive an electron density for the X-ray emitting gas in the remnant of $n_e = (0.1–0.2)(6 \text{ kpc}/D)^{1/2}$ cm^{-3}. This gas would have suffered at least one shock, hence the original ambient density would have been at most one fourth of this value. This is consistent with typical supernova energies and the observed size. Adopting an age of 16,000 yr and a radius of 33 pc for the remnant, and employing the Sedov solution (justified by the age of order 10^4 yr) we estimate the ratio E_{51}/n_0 at 40 (where E_{51} is the initial explosion energy in units of 10^{51} erg, and n_0 is the unperturbated ISM density in cm^{-3}). For $E_{51} \simeq 1$, we obtain $n_0 = 0.025$ cm^{-3} in good agreement with the density suggested by Finley & Ögelman. This is a very low value for the ISM density close to the galactic plane, suggesting that the SNR may be expanding inside a pre-formed cavity.

Alternatively, the pulsar-SNR association may not be valid, and the SNR may be older than the Σ-t relation suggests. The latter case would appear to be more conducive to triggered star formation, in part because more time would have elapsed during which star formation might have occurred, and in part because the supposition of a low density medium (in which star formation would be slower) is not necessary. The former case could still initiate star formation, of course, with the remnant expanding rapidly through a low density medium and then colliding with denser molecular clumps further from the blast site. In this case, we would expect the star formation to be in its earliest stages, and hence we would not detect many ultracompact H II regions.

Molecular gas has been detected toward the W30 SNR (Blitz, Fich, & Stark 1982; Bronfman et al. 1996). If the SNR is bounded on any side by a molecular cloud, then an interaction between the SNR and the cloud is expected. The 1720 MHz OH line traces shocked gas at the interface between SNRs and molecular clouds (Frail, Goss, & Slysh 1994) and hence might be present here. A single-dish survey by Goss (1968) failed to detect the line, however. This non-detection notwithstanding, an OH line study of W30, and possibly CO mapping, would be well-advised. More sensitive OH observations might show emission in the 1720 MHz line and CO maps would provide extremely valuable information on the ambient gas densities, which might help to explain the unusual morphology of the SNR (see, for example, Reynoso & Mangum 2001).

REFERENCES

Abbott, D. C., Bieging, J. H., Churchwell, E., & Cassinelli, J. P. 1980, ApJ, 238, 196

Altenhoff, W. J., Downes, D., Pauls, T., & Schraml, J. 1979, A&AS, 35, 23

Arendt, R. G. 1989, ApJS, 70, 181

Assousa, G. E., Herbst, W., & Turner, K. C. 1977, ApJ, 218, L13

Becker, R. H., White, R. L., Helfand, D. J., & Zoonematkermani, S. 1994, ApJS, 91, 347

Blitz, L., Fich, M, & Stark, A. A. 1982, ApJS, 49, 183

Bronfman, L., Nyman, L.-Å., & May, J. 1996, A&AS, 115, 81

Carral, P., Kurtz, S., Rodríguez, L. F., Martí, J., Lizano, S., & Osorio, M. 1999, RevMexAA, 35, 97

Caswell, J. L., & Lerche, I. 1979, MNRAS, 187, 201

Condon, J. J., Cotton, W. D., Greisen, E. W., Yin, Q. F., Perley, R. A., Taylor, G. B., & Broderick, J. J. 1998, AJ, 115, 1693

Finley, J. P. & Ögelman, H. 1994, ApJ, 434, L25

Frail, D. A., Goss, W. M., & Slysh, V. I. 1994, ApJ, 424, L111

Frail, D. A., Kassim, N. E., & Weiler, K. W. 1994, AJ, 107, 1120

Herbst, W., & Assousa, G. E. 1977, ApJ, 217, 473

Junkes, N., Fürst, E. & Reich, W. 1992, AA, 261, 289

Jura, M. 1976, AJ, 81, 178

Kassim, N. E. & Weiler, K. W. 1990, ApJ, 360, 184 (KW90)

Krebs, J., & Hillebrandt, W. 1983, AA, 128, 411

Kurtz, S., Churchwell, E., & Wood, D. O. S. 1994, ApJS, 91, 659

MacLeod, G. C., van der Walt, D. J., North, A., Gaylard, M. J., Galt, J. A., & Moriarty-Schieven, G. H. 1998, AJ, 116, 2936

Odegard, N. 1986, AJ, 92, 1372

Öpik, E. J. 1953, Irish Astron. J., 2, 219

Palla, F., Brand, J., Cesaroni, R., Comoretto, G, & Felli, M. 1991, A&A, 246, 249

Rengarajan, T. N., Verma, R. P., & Iyengar, K. V. K. 1989, MNRAS, 237, 1047

Reynoso, E. M., & Mangum, J. G., 2001, AJ, 121, 347

Taylor, J. H., Manchester, R. N., & Lyne, A. G. 1993, ApJS, 88, 529

Velázquez, P. F., Kurtz, S. E., Dubner, G. M., Goss, W. M., & Holdaway, M. A. 2002, AJ, submitted

Walsh, A. J., Burton, M. G., Hyland, A. R., & Robinson, G. 1998, MNRAS, 301, 640

Wink, J. E., Altenhoff, W. J., & Mezger, P. G. 1982, A&A, 108, 227

Wood, D. O. S. & Churchwell, E. 1989a, ApJ, 340, 265 (WC89a)

_____. 1989b, ApJS, 69, 831

Woodward, P. R. 1976, ApJ, 207, 484

Wouterloot, J. G. A., Brand, J., Burton, W. B., & Kwee, K. K. 1990, A&A, 230, 21

Zoonematkermani, S., Helfand, D. J., Becker, R. H., White, R. L., & Perley, R. A. 1990, ApJS, 74, 181

S. Jane Arthur, Stanley E. Kurtz, and Luis F. Rodríguez: Instituto de Astronomía, UNAM, Apartado Postal 3-72, 58090 Morelia, Michoacán, México (s.kurtz, l.rodriguez, j.arthur@astrosmo.unam.mx).

Pedro Ojeda-May: Facultad de Ingeniería, Universidad Autónoma de Yucatán, Periférico, Mérida, Yuc., México (pojeda@astrosmo.unam.mx).

Pablo F. Velázquez: Instituto de Ciencias Nucleares, UNAM, Apartado Postal 70-543, 04510 México, D. F., México (pablo@nuclecu.unam.mx).